AIRDOS – open source PIN diode airborne dosimeter

M. Kákona,[a,b,*] **J. Šlegl,**[a,b] **D. Kyselová,**[a,b] **M. Sommer,**[a,b] **J. Kákona,**[c] **M. Lužová,**[a,b] **V. Štěpán,**[a] **O. Ploc,**[a] **S. Kodaira,**[d] **J. Chroust,**[e] **D. John,**[b] **I. Ambrožová**[a] **and P. Krist**[a]

[a] *Nuclear Physics Institute of the Czech Academy of Sciences, Husinec - Řež 130, 250 68 Řež, Cech Republic*

[b] *Czech Technical University in Prague, Faculty of Nuclear Sciences and Physical Engineering, Břehová 7, 115 19 Prague, Czech Republic*

[c] *Czech Technical University in Prague, Faculty of Electrical Engineering, Technická 2, 166 27 Prague, Czech Republic*

[d] *National Institutes for Quantum and Radiological Science and Technology, 4-9-1 Anagawa, Inage-ku, Chiba 263-8555, Japan*

[e] *Universal Scientific Technologies, Soběslav, Czech Republic*

E-mail: martin.kakona@odz.ujf.cas.cz

ABSTRACT: This article introduces a new open-source dosimeter AIRDOS intended for measurements on board aircraft. Measurement of a mixed radiation field on board aircraft is a challenging deal with needs of a small, low power consumption, battery operated, lightweight device with long endurance. The new innovative electronic design with silicon PIN diode as a sensor with full described design including manufacturing documentation is introduced. This device was verified by measurements and compared with reference dosimeters widely used in aircraft dosimetry as Liulin MDU and HAWK TEPC. The comparison of measurements with a computation model CARI 7 was performed as well. All those comparisons give good results within known errors. The new design of the dosimeter has very good performance in endurance on battery and does not need calibration after manufacturing and recalibration after long time usage. Open-source design predetermines AIRDOS for future improvements and for open-science.

KEYWORDS: PIN diode dosimeter; silicon diode dosimeter; airborne dosimeter; dosimetry on board aircraft.

* Corresponding author.

Contents

1. Introduction

Our group has been performing routine measurements of ionizing radiation on board aircraft by silicon diode based dosimeter Liulin since 2001 [1]. These measurements were compared with the measurements of secondary cosmic rays performed on the ground by neutron monitors [2] and with a model of secondary cosmic rays CARI [3] which is used for the estimation of aircrew doses in the Czech Republic [4]. Our effort in long-term measurements [5] has resulted in the development of a new dosimeter with fully described design. Our motivation was comprehension of mechanisms inside dosimeter electronics. Because last years many people spent a lot of effort redesigning a silicon dosimeter from scratch [6–9] our aim was introducing an open-source, fully documented design which can be used as a base platform for the future improvements and modifications for the desired deployment. This newly developed airborne dosimeter, called AIRDOS, has comparable properties as Liulin dosimeter [10], which enables the continuation of our long term measurements on board aircraft and introduces new features like calibration stability and long battery operation.

The AIRDOS is intended for measurements in low intensity mixed ionizing radiation fields. In its aircraft version, it houses a silicon PIN diode as a radiation detector, an electronics for conversion of the signal to the pulse-height spectra, a GPS module (optional), a datalogger, a memory card and batteries for up to six months of operation. It is a portable device for routine measurements on board aircraft. This design is built on an Open Hardware modular platform MLAB, the firmware is written in Open Software platform Processing and data processing is

written in Python using Open Software scientific libraries. Manufacturing documentation, firmware documentation and scripts for data evaluation for this dosimeter are publicly available at GitHub server [11, 12].

Measurements with AIRDOS onboard aircraft during several individual flights were compared with computational model and also with measurements with other devices.

2. AIRDOS design

2.1 Hardware design

AIRDOS is a low power, battery operated, absorbed dose in silicon spectrometer. It contains a silicon PIN diode (Hamamatsu S2744-09) as a sensor, analog signal processing and acquisition unit with datalogger. Optionally, a GPS (Global Positioning System) receiver is mounted. Two LS33600 (Li-SOCl2) cells are used as a power source. The endurance of measurement is six months without GPS and one month with GPS. The data are stored on an SD card (Secure Digital Memory Card). Block schematic of AIRDOS is depicted in figure 1 and a typical outfit with an aluminium case is shown in figure 2. Electronics is divided into two, respectively three PCB's (Printed Circuits Boards): analog electronics (PCRD04B), the GPS receiver (GPS01B) and a datalogger (DATALOGGER01A). See figure 3. The dosimeter modules have become a part of an Open Hardware project MLAB [13]. All modules are available under GNU General Public License v3.0 [14]. The modularity of AIRDOS allows further development, easy adding of new features, easy adding of new sensors and a cooperation with the open hardware project.

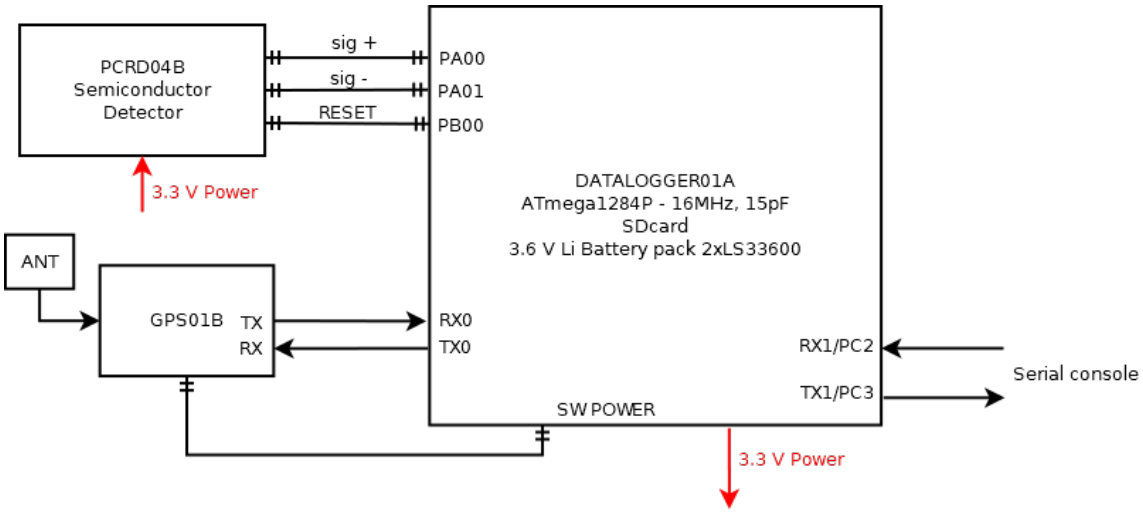

Figure 1. Block diagram of AIRDOS 02.

Figure 2. Outfit of AIRDOS 02 dosimeter.

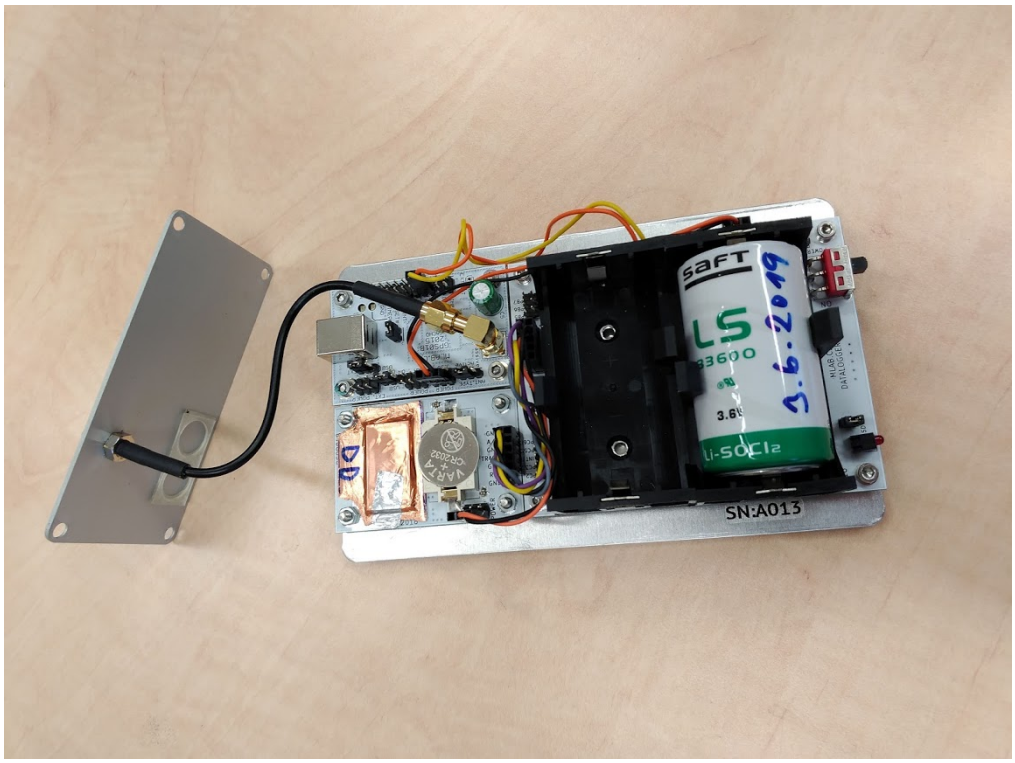

Figure 3. Deployment of PCB's inside the AIRDOS 02 dosimeter. In centre down is the analog frontend with a PIN diode sensor covered by copper sheet and a V_{bias} battery CR2032. Module with connected coaxial cable is the GPS.

2.2 Analog circuit design

All analog circuits are implemented on PCB (Printed Circuits Board) PCRD04B. Manufacturing documentation for this module is available on-line [15].

Silicon PIN photodiode (D2) is connected to a trans-impedance amplifier (figure 4) and is negatively biased by lithium cell CR2032 (BT1) with 3 V against the reference voltage REF 1.2 V.

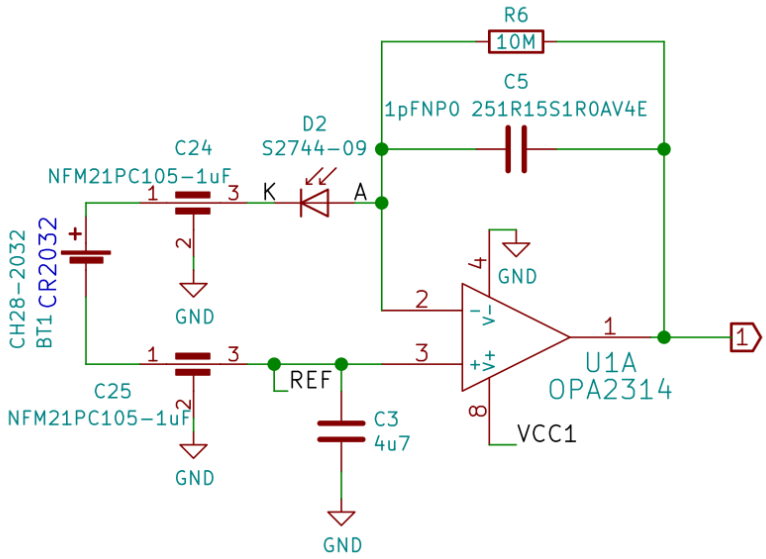

Figure 4. Silicon PIN diode sensor and charge amplifier / trans-impedance amplifier.

Voltage signal from the trans-impedance amplifier is filtered by a bandpass filter. For more information see [15]. Each ionizing radiation event in the photodiode produces, after filtering/shaping, a pulse with a duration of about 80 µs. The amplitude of the pulse is proportional to charge in case of a constant charge collection time and the charge is proportional to the deposited energy in a sensitive volume in the PIN diode.

Resulting pulses are stored in a specially developed sample-hold circuit that behaves as a signal follower and analog memory (figure 5). When signal #PeakDetect_Trace is in H an analog switch U5 turns on and a signal at an output U2B follows a signal at input (2) with slight delay which is done by R13 and C19. If signal #PeakDetect_Trace is switched to a high impedance state the analog switch U5 starts to be controlled by a comparator U4. In this case, when the input signal (2) goes from high to low, a positive input of comparator will be at a higher voltage than negative input, following a voltage at capacitor C19. It causes switching-off of the analog switch U5 and the capacitor C19 holds its last voltage value. This behaviour is similar to a peak detector circuit. Next the stored voltage can be converted by ADC (Analogue to Digital Converter) and after this conversion the input #PeakDetect_Trace goes again to H and circuit changes behavior to signal follower circuit. The described sample-hold circuit does not suffer with typical peak detector circuits ills like insensitivity to small signals, mistreatment of negative signals or discharging the capacitor by leakage current through diodes. Moreover, this circuit can be used as a pulse discriminator as well. The signal #PeakDetect_Trace can be connected to an input of digital circuits when it is controlled by the comparator U4. When the

input signal (2) goes from high to low, the signal #PeakDetect_Trace goes from high to low as well. This behaviour can be used for detection of a falling edge of signal. There is only one constraint of this circuit, the input signal can not change raising/falling time widely and RC time constant (R13, C19) must be chosen correctly, respecting the input signal time properties.

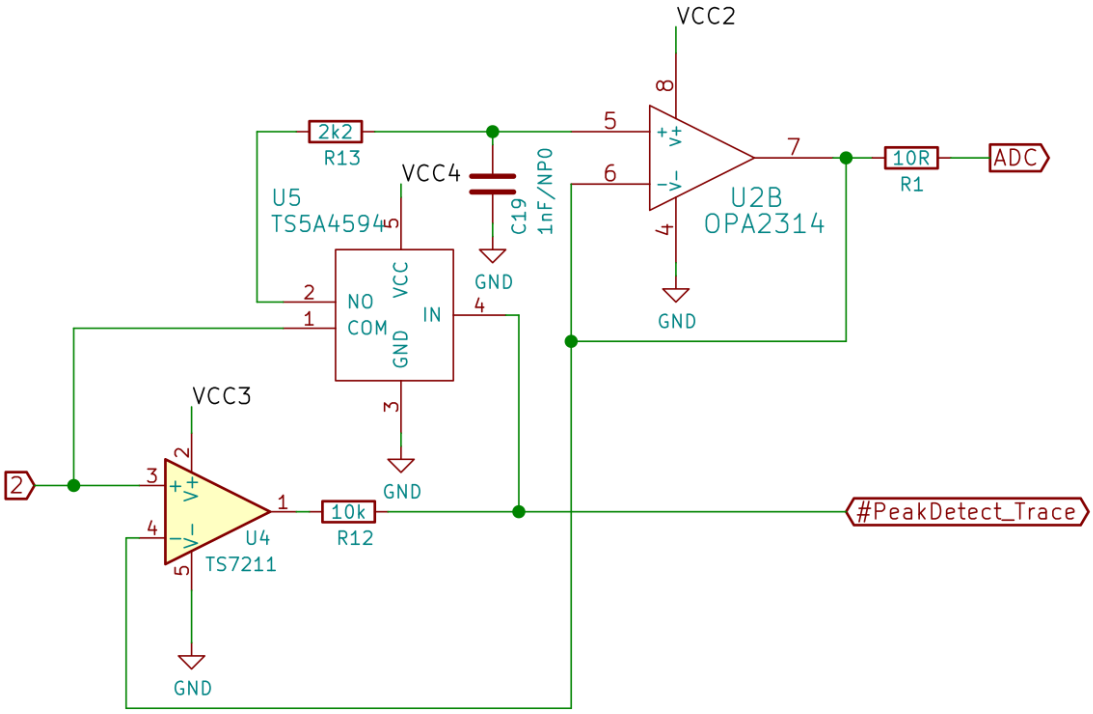

Figure 5. Signal follower with analog memory. It is a circuit equivalent to a sample-hold circuit triggered by a falling edge of signal or a circuit equivalent to a peak detector.

2.3 Digital circuit design

A data acquisition unit is based on DATALOGGER01A module. Manufacturing documentation for this module is available on-line [16]. ATmega 1284P [17] a single chip µC (microcomputer) was used. This µC is a low power variant of ATmega 1284 and utilises differential 10-bit ADC (Analog to Digital Converter). Power consumption of this µC is less than 1 mA on working frequency 1 MHz (AIRDOS does not use an external crystal oscillator). Each manufactured AIRDOS contains a silicon serial number. This serial number is used as a marker for output data and helps registration of deployment of dosimeters and data pairing with specific aircraft.

The rest of the electronics comprises an RTC (Real Time Clock) with an accuracy of 20 PPM, a power switch for switching-off the GPS and an SD card slot. The whole SD card is switched-off during the dosimeter integration as well as the power for the GPS. Power for the SD card and GPS is controlled by firmware.

2.4 AIRDOS Firmware design

The firmware of AIRDOS was written in Processing language environment [18] for ease of modification by non-programmers (e.g. scientists). Source code of the firmware is available under GNU General Public License v3.0 on GitHub [19].

There is no signal discriminator in AIRDOS hardware. Consequently, AIRDOS firmware periodically samples the analog signal. This sampling is asynchronous with ionization events and one event can accidentally belong to two neighboring samples. This circumstance has to be solved by a software filter. Filtering algorithm is described in figure 6. This algorithm is looking for local maxima of signal and stores these local maxima to an array Histogram[].

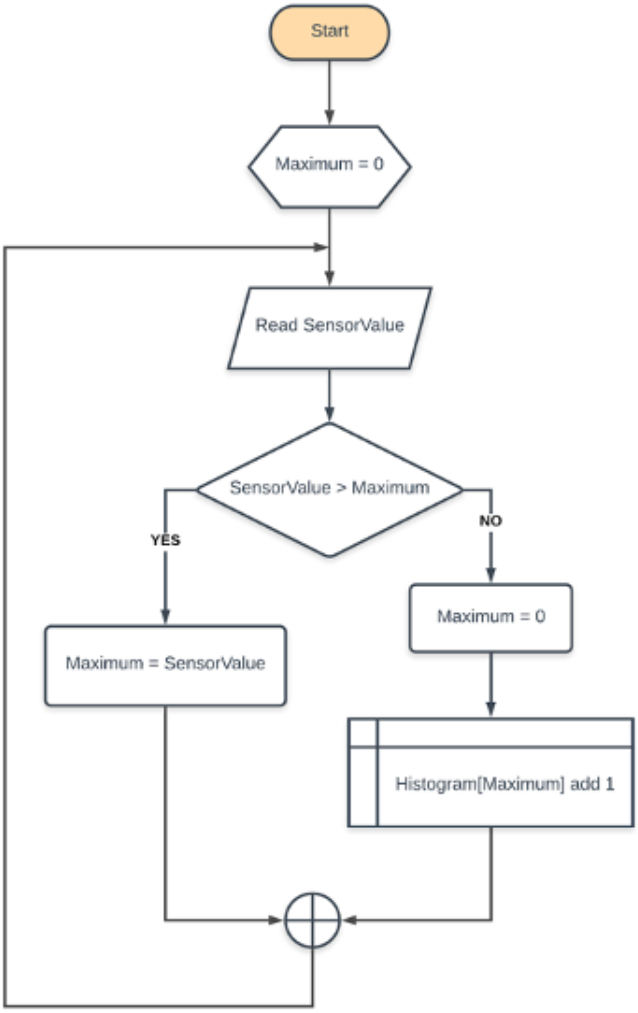

Figure 6. Flowchart of algorithm for suppressing a double detection of events. SensorValue is a value obtained from ADC. Maximum is a local variable. Histogram variable is an array for output values sorted by deposited energy (in channels).

2.5 AIRDOS Output

Data from AIRDOS can be obtained by an asynchronous serial protocol at UART (Universal Asynchronous Receiver/Transmitter) interface or can be stored on SD card. Data format is described in protocol documentation at [20]. Parsers for output data are also available as an open source code at [21].

3. AIRDOS Calibration

3.1 Energy calibration

Energy response was investigated using a defined charge injected through a calibrated capacitor 1 pF (C_T) connected to a signal generator (figure 7).

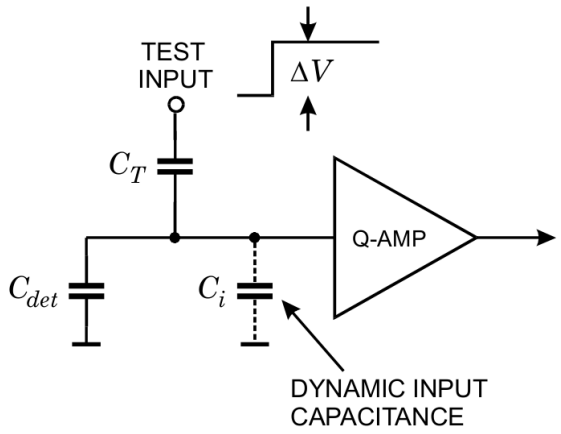

Figure 7. Circuit for calibration [22].

The slope of rising edge of generated pulses was set to be equal to real pulses from ionisation events. The amplitude of voltage pulses (ΔV) was measured by an oscilloscope and charge was calculated using a formula

$$Q = \Delta V C_T$$

where Q is charge in Coulombs, C_T is capacity in Farads and ΔV is voltage in Volts. This formula is true in case $C_i >> C_T$. Capacity of photodiode C_{det} is two orders higher than our 1 pF capacitor (C_T) - therefore, in our case, this condition is fulfilled.

Now we can easily calculate the number of electrons corresponding to injected charge.

$$N_e = \frac{Q}{e}$$

where N_e is the number of electrons, Q is charge and e is the elementary charge (1.602×10^{-19} C).

Then, the estimated ionisation energy corresponds to the number of electron-hole pairs

$$E = N_e \varepsilon_{e-h}$$

where E is the energy in eV deposited by ionising radiation, N_e is the number of released electrons and $\varepsilon_{e\text{-}h}$ is equal to 3.65 eV for silicon and it represents mean energy for electron-hole pair creation.

Figure 8 shows the result of energy calibration by injected charge. As can be seen the response is perfectly linear.

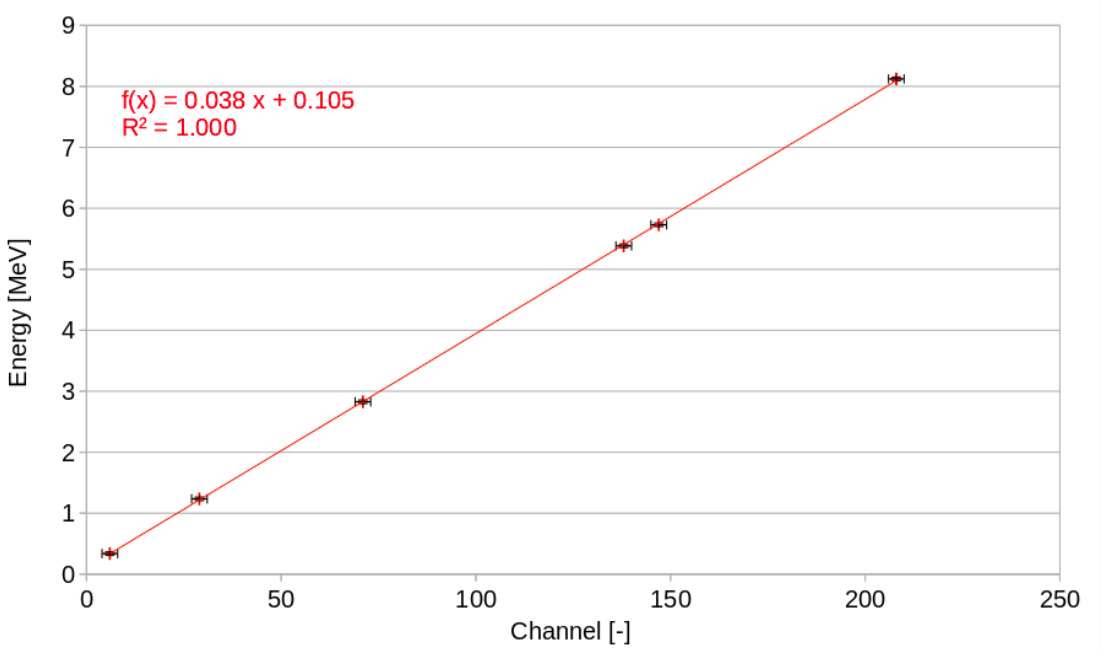

Figure 8. Energy response obtained by injecting a defined charge into the input of charge amplifier. Depicted error bars display quantisation error of ADC.

The second method of energetic calibration is a measurement of response to real ionising particles originating in radioactive nuclides or particle accelerators. Summary of ions used for the calibration is in table 1.

Alphas from radionuclide sources as representatives of heavy ions particles and protons and alphas from accelerators as representatives of particles with weak interaction with the sensor were used for energy calibration of AIRDOS. This selection covers almost all the detector's energy range (from 0.2 MeV to 9 MeV). Deposited energies were calculated by SRIM program [23,24]. Figure 9 presents responses for alpha particles from radionuclide sources (^{239}Pu, ^{241}Am), alpha particles from HIMAC (Heavy Ion Medical Accelerator in Chiba) accelerator [25] and protons from U-120M accelerator [26]. From this figure it can be seen that measured energies from real particles slightly differ from the method of injected charge presented above. It should be noted that the real particles have to give theoretically lower values because of energy loss in an entrance window of the detector, limited lifetime of charge carriers and slower charge collection speed. However, we observed positive offset which can be attributed to the noise of the detector. This noise is caused mainly by a current noise of the input of the trans-impedance amplifier and thermal noise/dark current of the diode. This noise is proportional to the internal capacity of the photodiode and is negligible in case of charge injected by capacitor because capacity of the sensor is two orders higher than the capacity of the capacitor used for injecting charge.

Four manufactured AIRDOS dosimeters were checked by the method of injected charge through a capacitor, the differences in calibration between individual units are less than one channel of ADC. We can conclude that the calibration of individual devices is not necessary.

Table 1. Table of ions used for AIRDOS energy calibration.

Source name	**Origin**	**Calculated Deposited Energy in 300 µm of Si [MeV]**
He150	HIMAC Helium 150 MeV/u	1.3
He150 + BF 1	HIMAC Helium 150 MeV/u with filter equivalent to 127.68 mm H_2O	2.8
He150 + BF 2	HIMAC Helium 150 MeV/u with filter equivalent to 142.02 mm H_2O	4.7
p+	U-120M Protons 35 MeV (31 MeV in place of detector)	1.0
p+ (3 + 4)	U-120M Protons 35 MeV with Al filters (3.14 mm of Al and 2000 mm of air)	1.7
Pu	Calibration alpha source EA14 AMPU 14 with ^{239}Pu and ^{241}Am	5.2
Am	Calibration alpha source EA14 AMPU 14 with ^{239}Pu and ^{241}Am	5.5

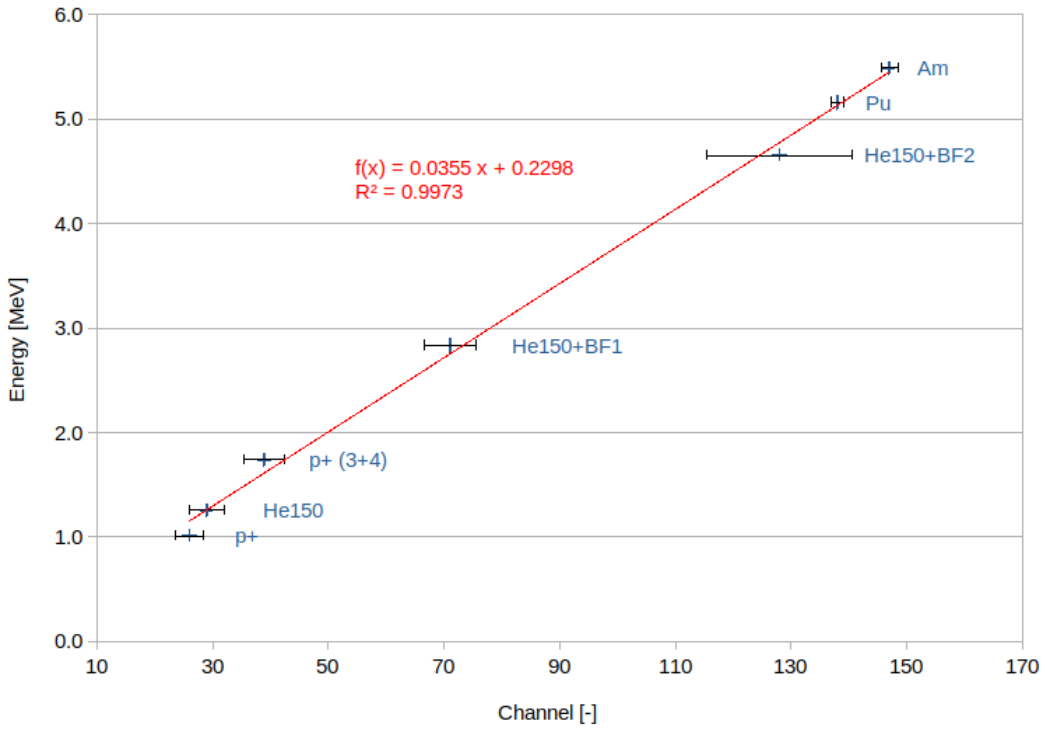

Figure 9. Energetic calibration of AIRDOS. Depicted errors are FWHM values. Used ions are described in table 1.

3.2 Thermal stability

Thermal stability of AIRDOS was tested with alpha particles from ^{241}Am and ^{239}Pu radionuclide thin layer calibration sources during cooling in the refrigerator in the temperature range from +20°C to -15°C. The difference in temperature resulted in the difference in detected deposited energy is in scale of one channel (38 keV) per 12 °C. This temperature dependence is negligible for the intended use of the detector on board the air conditioned commercial aircraft.

3.3 Flux calibration

AIRDOS dosimeter detects all particles up to the flux that does not cause pile-ups. Since AIRDOS is intended for the use on board aircraft where the fluxes are very low with respect to the used diode area the pile-ups are very rare. Therefore the calibration to the flux is not needed. Only dead time must be taken into account. There are two types of dead time in AIRDOS, time for writing data to SD card and time for obtaining absolute time and position information from GPS. These periods should vary slightly depending on GPS signal quality or internal file system conditions of SD card. Nevertheless, integration time of one measurement cycle (time for collecting data to histogram before writing to SD card) is constant and is specifically 10.4 s. ADC performs 46000 samples during this period. Timeout for waiting for GPS signal is 58 s. Time for writing to SD card alternates from 2 to 4 s depending on SD card type and condition. We can conclude that the number of events/particles in one measurement cycle must be divided by 10.4 for obtaining the rate per second. The time needed for writing to the SD card and for obtaining position for GPS is, in fact, dummy time without measurement and can not be calculated to the output rates.

When we want to obtain cumulative dose in silicon D_{Si}, we have to use equation

$$D_{Si} = \frac{t_{meas}}{10.4n} \sum_{i=1}^{n} d_i$$

when d_i is a dose measured during one integration period recorded in the device datalog, t_{meas} is time of the whole measurement performed by AIRDOS in seconds and n is the number of measurements performed during the measurement period t_{meas}.

4. Results

Finally reached parameters of the design of AIRDOS are summarised in table 2. Compared to parameters of Liulin dosimeter [7] AIRDOS does not need calibration after manufacturing and there is no problem with first energy channels, because of different analog circuits design and omitting the comparator (signal discriminator). These new features were proven by measurements described below. The last feature is the increase in operation time on batteries more than twice.

Table 2. Parameters of AIRDOS dosimeter (for version 02 F).

Dimensions	166 x 107 x 57 mm^3
Weight	730 g
Energy range	from 0.2 to 9 MeV
Number of channels	240
Channel width	38 keV
Integration time	10.4 s
Continuous measurement	6 months
PIN diode type	Hamamatsu S2744-09
Battery	2x LS 33600
Memory	SD card

Results obtained with AIRDOS were compared with Liulin dosimeter [7] in selected flight and long term measurement at high mountain observatory [27]. Differences in cumulative dose in silicon measured by Liulin and AIRDOS during the whole measurement campaign were below 10 % with systematic error +4.8 % [27]. Please note that this comparison was done for deposited energies above 250 keV. It is due to different designs of Liulin and AIRDOS dosimeters because Liulin dosimeter uses a signal discriminator/comparator which introduces jitter to first channels (lower energies) and different pieces of Liulin show different settings of the comparison level. Therefore these channels were omitted in comparison.

For assessment of radiation exposure onboard aircraft measured by AIRDOS, the flight from Prague (PRG; Cutoff Rigidity = 3.5 GV) to Malaga (AGP; Cutoff Rigidity = 8.6 GV) and back was performed. Measurement campaign lasted from 2019-11-28 16:00 to 2019-11-29 01:10 UTC and for calculation of dose the time from 2019-11-28 18:55 to 2019-11-28 20:55 was used for the flight PRG-AGP and from 2019-11-28 23:00 to 2019-11-29 00:30 for the flight AGP-PRG when the aircraft was at nominal flight level. The data from three different AIRDOS devices (with serial numbers 16, 21 and F0) were used.

Calculation of an effective dose during the flight was done by CARI 7 computer program [28]. CARI 7 uses a database of atmospheric response which is generated by Monte Carlo particle transport program MCNPX 2.7.0. Modulation of cosmic rays by the solar wind is taken into account by the monthly averages of the heliospheric potential available at FAA (Federal Aviation Administration) web site [28, 29].

Since the effective dose is not a measurable quantity, an ambient dose equivalent $H^*(10)$ was introduced [30]. For calculation of an ambient dose equivalent rate from a dose rate in silicon provided by AIRDOS, we used the approach described in [31]. This method was established for Liulin, nevertheless AIRDOS utilises the exactly same PIN diode as Liulin thus dose in silicon has to be same. Liulin has different energy range but particles with deposited energy higher than 9 MeV are rare on board aircraft (we encountered only 9 events over the range during both flights which represents less than 3 % of ambient dose equivalent) and lower channels (with deposited energy < 200 keV) are usually omitted in Liulin data.

First, we have to calculate the dose rate in silicon

$$\frac{dD_{Si}}{dt} = \frac{\sum_{i=4}^{250} 0.038 N_i + 0.105}{m_{Si} \Delta t}$$

where coefficients (0.038 and 0.105) are taken from the fit in figure 8, m_{Si} is 0.1398 g [32,33] and integration time Δt is 10.4 s. N_i is the number of events registered in channel i.

Then we apply coefficients for conversion dose in silicon to ambient dose equivalent

$$\frac{dH^*(10)}{dt} = \frac{dD_{Si}}{dt} k_{Liulin/Airdos} k_{Sv/Gy}$$

where, $k_{Liulin/Airdos}$=1.05, it represents different channel width of Liulin and AIRDOS and this systematic difference is estimated as 5 % (lowest estimation of this systematic difference is 4.8 % by [27]), $k_{Sv/Gy}$=2.45, it is a mean value of a calibration factor for Liulin by the work [31] for the geomagnetic cutoff rigidities from 3.5 to 8.6 GV. Calculated values for the three AIRDOS devices are displayed in the graphs in figure 10 for the specific flight. We can see change of measured value corresponding to calculation during moving a plane respecting changing the flight level and traveling through regions with different geomagnetic rigidities in time (from north to south during the flight PRG-AGP and from south to north during the flight AGP-PRG).

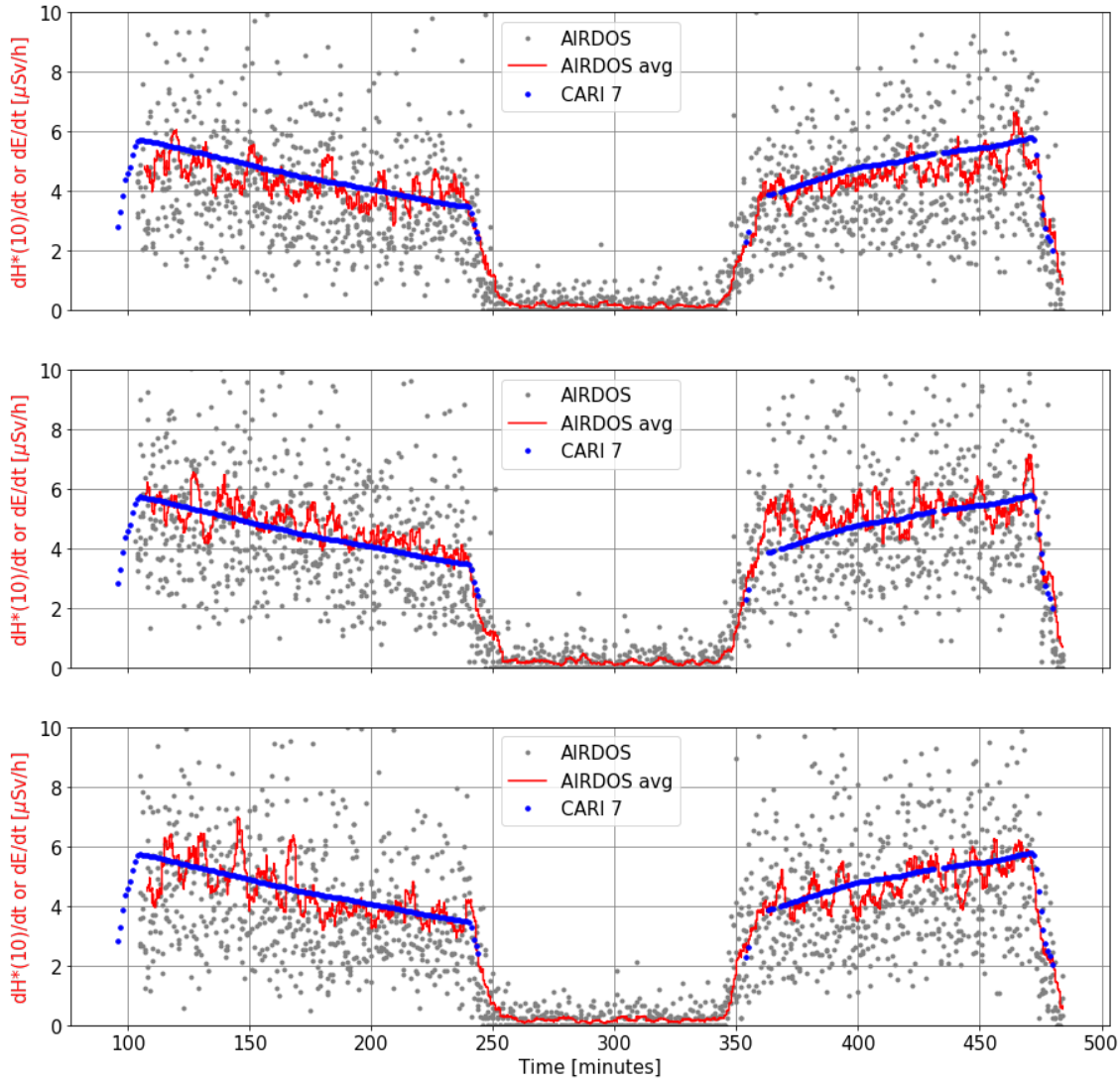

Figure 10. Radiation profiles of flights PRG-AGP (left) and AGP-PRG (right) in time. Gray points are particular measurements recalculated to ambient dose equivalent rate. Each measurement lasted 10.4 s. Red curves are running averages for 20 measurements. Blue dots are effective dose rates calculated by CARI 7 according to the flight route. Measurements were performed with AIRDOSes with serial numbers 16, 21 and F0 from the top to bottom.

5. Discussion

In table 3 we compare the measured/calculated ambient dose equivalent (by AIRDOS) with an effective dose calculated by CARI 7. Despite the fact that the general calibration fit (from Figure 8) was used and calibration for individual manufactured AIRDOSes has not been taken into account, the errors in ambient dose equivalent are mostly less than 10 %. Differences between the devices are mostly due to a DC offset of the A/D converter. This offset is compensated in the firmware but the compensation can be done with granularity of one channel

width only (i.e. about 38 keV). This compensation is done according to chapter Offset Compensation Schemes in a datasheet [17].

Together with AIRDOSes we performed measurement with TEPC (Tissue-Equivalent Proportional Counter) HAWK FW-AD1 dosimeter [34]. The calculated ambient dose equivalents provided by HAWK measurements are included in table 3 as well. Again the measured values are within the error of 10 % in comparison of CARI 7 calculations which is in acceptable error by manufacturer's documentation for HAWK TEPC and by the other literature [35].

We have to add a note about quantities used for the comparison. The effective dose E [30] provided by CARI 7 cannot be directly measured therefore we use the ambient dose equivalent $H^*(10)$ [30] for the AIRDOS measurements. The ambient dose equivalent is commonly used as a conservative estimation of the effective dose in case of isotropic radiation [36]. It should be also mentioned that there are other approaches how to determine calibration coefficients for converting D_{Si} to $H^*(10)$, for example [37].

Table 3. Comparison of doses calculated by CARI 7 program and doses measured with three manufactured dosimeters and TEPC. Please note that error of the used computation method [31] of the ambient dose equivalent is ±2.6 % and CARI 7 model deviation from ICRU reference data is from -4 % to +14 % [3]. The overall uncertainty of values provided by HAWK is 10% [35].

	PRG-AGP		**AGP-PRG**	
Program or Dosimeter	**H*(10) or E [μSv]**	**Difference**	**H*(10) or E [μSv]**	**Difference**
CARI 7	8.7	reference value	7.6	reference value
Hawk TEPC	9.4	+8.0 %	8.1	+6.6 %
AIRDOS s.n. 16	8.8	+1.1 %	7.3	-3.9 %
AIRDOS s.n. 21	8.1	-6.9 %	6.8	-10.5 %
AIRDOS s.n. F0	9.2	+5.7 %	7.7	+1.3 %

6. Conclusions

A new open-source dosimeter for measurements on board aircraft was introduced. AIRDOS dosimeter was tested in the real radiation field on board aircraft and obtained results corresponding with simulations and comparison measurements. It is the first step towards future improvements and innovations originated in the public scientific community based on a fully described open-source design. We share our effort for better understanding of solid-state dosimeters. We hope that we encourage other scientists and designers to introduce their ideas to open-science in mixed radiation field dosimetry.

Acknowledgments

I would like to thank Mikhail A. Mikhailov for providing calibrated capacitors and for guiding me through practical detector calibration.
This work was supported by EU Operational Program Research, Development, and Education in project CRREAT (CZ.02.1.01/0.0/0.0/15_003/0000481). Measurements were carried out at CANAM infrastructure of the NPI CAS Rez supported through MEYS project No. LM2015056 and at HIMAC under project H377.

References

[1] Ploc, O., Ambrozova, I., Kubancak, J., Kovar, I., & Dachev, T. P. (2013). Publicly available database of measurements with the silicon spectrometer Liulin onboard aircraft. Radiation measurements, 58, 107–112. doi:10.1016/j.radmeas.2013.09.002

[2] Kákona, M., Ploc, O., Kyselová, D., Kubančák, J., Langer, R., & Kudela, K. (2016). Investigation on contribution of neutron monitor data to estimation of aviation doses. Life Sciences in Space Research, 11, 24–28. doi:10.1016/j.lssr.2016.11.001

[3] Copeland, K. (2017). Cari-7a: development and validation. Radiation Protection Dosimetry, 175(4), 419–431. doi:10.1093/rpd/ncw369

[4] Kubančák, J., Kyselová, D., Kovář, I., Hlaváčová, M., Langer, R., Strhársky, I., … Ploc, O. (2019). Overview of aircrew exposure to cosmic radiation in the czech republic. Radiation Protection Dosimetry. doi:10.1093/rpd/ncz204

[5] Kákona, M., Kyselová, D., Ambrožová, I., Kubančák, J., Štěpán, V., Langer, R., … Ploc, O. (2019). CR10 - a public database of cosmic radiation measurements at aviation altitudes of about 10 km. Radiation Protection Dosimetry. doi:10.1093/rpd/ncz207

[6] Dachev, T., Dimitrov, P., Tomov, B., & Matviichuk, Y. (2001). TECHNICAL DESCRIPTIONOF LIULIN-4 TYPE LET SPECTROMETERS (LETS) . Retrieved from http://citeseerx.ist.psu.edu/viewdoc/download?doi=10.1.1.504.2611&rep=rep1&type=pdf

[7] Dachev, T., Dimitrov, P., Tomov, B., & Matviichuk, Y. (2009). Technical Description of the Spectrometer-Dosimeter Liulin-6C MDU-6.

[8] Ritter, B., Maršálek, K., Berger, T., Burmeister, S., Reitz, G., & Heber, B. (2014). A small active dosimeter for applications in space. Nuclear Instruments and Methods in Physics Research Section A: Accelerators, Spectrometers, Detectors and Associated Equipment, 748, 61–69. doi:10.1016/j.nima.2014.02.030

[9] Berger, T., Marsalek, K., Aeckerlein, J., Hauslage, J., Matthiä, D., Przybyla, B., … Wirtz, M. (2019). The German Aerospace Center M-42 radiation detector-A new development for applications in mixed radiation fields. The Review of scientific instruments, 90(12), 125115. doi:10.1063/1.5122301

[10] Dachev, T., Tomov, B., Matviichuk, Y., Dimitrov, P., Lemaire, J., Gregoire, G., … Spurny, F. (2002). Calibration results obtained with Liulin-4 type dosimeters. Advances in Space Research, 30(4), 917–925. doi:10.1016/S0273-1177(02)00411-8

[11] Kákona, M., Chroust, J., Kákona, J., Lužová, M., Kyselová, D., Šlegl, J., … Krist, P. (2017). AIRDOS01. Retrieved January 1, 2020, from https://github.com/ODZ-UJF-AV-CR/AIRDOS01

[12] Kákona, M., & Chroust, J. (2018). AIRDOS02. Retrieved January 1, 2020, from https://github.com/ODZ-UJF-AV-CR/AIRDOS01

[13] MLAB. (2003). MLAB project. MLAB. Retrieved January 8, 2020, from https://mlab.cz/

[14] GNU. (2007). GNU General Public License v. 3.0. GNU General Public License. Retrieved January 8, 2020, from https://www.gnu.org/licenses/gpl-3.0.en.html

[15] Kákona, M. (2018). PCRD04B. MLAB. Retrieved January 1, 2020, from https://github.com/MLAB-project/Modules/tree/master/sensors/PCRD04B

[16] Kákona, M., & Chroust, J. (2018). DATALOGGER01A. MLAB. Retrieved January 1, 2020, from https://github.com/MLAB-project/Modules/tree/master/sensors/DATALOGGER01A

[17] Microchip. (2018). ATmega164A/PA/324A/PA/644A/PA/1284/P, (ISBN: 978-1-5224-3637-9).

[18] Processing Foundation. (2001). Processing language. Retrieved January 9, 2020, from https://processing.org/

[19] Kákona, M. (2018). AIRDOS Firmware. GitHub AIRDOS firmware. Retrieved January 1, 2020, from https://github.com/ODZ-UJF-AV-CR/AIRDOS02/tree/AIRDOS02A/sw

[20] Kákona, M. (2019). AIRDOS data format. GitHub AIRDOS wiki. Retrieved January 1, 2020, from https://github.com/ODZ-UJF-AV-CR/AIRDOS01/wiki/AIRDOS-data-format

[21] Kákona, M. (2017). AIRDOS data parser. GitHub AIRDOS parser. Retrieved January 1, 2020, from https://github.com/ODZ-UJF-AV-CR/AIRDOS-parser

[22] Spieler, H. (2012). Silicon Detectors. IEEE 2012 Nuclear Science Symposium, Medical Imaging Conference.

[23] Ziegler, J. F. (2010). SRIM. Retrieved January 5, 2020, from http://www.srim.org/index.htm

[24] Ziegler, J. F., Ziegler, M. D., & Biersack, J. P. (2010). SRIM – The stopping and range of ions in matter (2010). Nuclear Instruments and Methods in Physics Research Section B: Beam Interactions with Materials and Atoms, 268(11–12), 1818–1823. doi:10.1016/j.nimb.2010.02.091

[25] Yamada, S. (1995). Commissioning and performance of the HIMAC medical accelerator. In Proceedings Particle Accelerator Conference (pp. 9–13). Presented at the Particle Accelerator Conference, IEEE. doi:10.1109/PAC.1995.504557

[26] Křížek, F., Ferencei, J., Matlocha, T., Pospíšil, J., Príbeli, P., Raskina, V., … Vysoká, K. (2018). Irradiation setup at the U-120M cyclotron facility. Nuclear Instruments and Methods in Physics Research Section A: Accelerators, Spectrometers, Detectors and Associated Equipment, 894, 87–95. doi:10.1016/j.nima.2018.03.066

[27] Kákona, M., Štěpán, V., Ambrožová, I., Arsov, T., Chroust, J., Kákona, J., … Angelov, C. (2019). Comparative measurements of mixed radiation fields using liulin and AIRDOS dosimeters (Vol. 2075, p. 130003). Presented at the 10th Jubilee International Conference of the Balkan Physical Union, Author(s). doi:10.1063/1.5091288

[28] Copeland, K., Friedberg, W., Duke, F., Snyder, L., O'Brien, K., Parker, D., … Smart, D. (2017, June 6). CARI 7. Computer program CARI-7. Retrieved December 8, 2019, from https://www.faa.gov/data_research/research/med_humanfacs/aeromedical/radiobiology/cari7/

[29] FAA. (2019). Heliocentric potential. Retrieved January 1, 2020, from https://www.faa.gov/data_research/research/med_humanfacs/aeromedical/radiobiology/heliocentric/

[30] ICRP. (2007). ICRP Publication 103, The 2007 Recommendations of the International Commission on Radiological Protection. Annals of the ICRP.

[31] Wissmann, F., & Klages, T. (2019). A simple method to monitor the dose rate of secondary cosmic radiation at altitude. Journal of radiological protection : official journal of the Society for Radiological Protection, 39(1), 71–84. doi:10.1088/1361-6498/aaeeae

[32] Meier, M. M., Trompier, F., Ambrozova, I., Kubancak, J., Matthiä, D., Ploc, O., … Wirtz, M. (2016). CONCORD: comparison of cosmic radiation detectors in the radiation field at aviation altitudes. Journal of Space Weather and Space Climate, 6, A24. doi:10.1051/swsc/2016017

[33] Uchihori, Y., Kitamura, H., Fujitaka, K., Dachev, T. P., Tomov, B. T., Dimitrov, P. G., & Matviichuk, Y. (2002). Analysis of the calibration results obtained with Liulin-4J spectrometer-dosimeter on protons and heavy ions. Radiation measurements, 35(2), 127–134. doi:10.1016/s1350-4487(01)00286-4

[34] Far West Technology, Inc. (2010). "HAWK" TEPC ENVIRONMENTAL MONITOR MODEL FW-AD1. Retrieved January 1, 2020, from https://www.fwt.com/detector/fw-ad1ds.htm

[35] Farah, J., De Saint-Hubert, M., Mojżeszek, N., Chiriotti, S., Gryzinski, M., Ploc, O., … Olko, P. (2017). Performance tests and comparison of microdosimetric measurements with four tissue-equivalent proportional counters in scanning proton therapy. Radiation measurements, 96, 42–52. doi:10.1016/j.radmeas.2016.12.005

[36] ICRU. (2010). Report 84. Journal of the ICRU, 10(2), NP-NP. doi:10.1093/jicru/10.2.Report84

[37] Ploc, O., Pachnerová Brabcová, K., Spurny, F., Malušek, A., & Dachev, T. (2011). Use of energy deposition spectrometer Liulin for individual monitoring of aircrew. Radiation Protection Dosimetry, 144(1–4), 611–614. doi:10.1093/rpd/ncq505